Time-Resolved UV Resonance Raman Detection of a Transient Open Form of the Ligand Pathway in Tyr64(E7) Myoglobin

Masahiro Mukai,[†] Satoru Nakashima,[†,§] John S. Olson,[‡] and Teizo Kitagawa*[,†]

Institute for Molecular Science, Okazaki National Research Institutes, Myodaiji, Okazaki, 444 Japan, and Department of Biochemistry and Cell Biology, Rice University, Houston, Texas 77251, U.S.A.

Received: November 4, 1997; In Final Form: February 25, 1998

X-ray crystallographic analyses of myoglobin (Mb) in the deoxy and CO-bound states noted the absence of a preformed pathway for ligand movement from the heme iron to the solvent. To explore a mechanism of ligand entry, time-resolved UV resonance Raman experiments have been carried out, using a mutant with tyrosine at the distal histidine position. The results indicate the presence of a transient, open pathway which is generated after photodissociation of CO in the H64Y mutant. The Raman spectra were probed at 235 and 416 nm with a time resolution of 7 ns in the range −100 ns to 10 ms following photolysis at 532 nm. In the 235 nm excited spectra, the tyrosine bands of H64Y Mb at 1618 (Y8a) and 1176 cm^{-1} (Y9a) are noticeably intensity-enhanced shortly after photolysis, but the original intensity is restored by 5 ms. The time range in which the Tyr bands are intensified is prolonged by addition of glycerol to the solvent. This intensity change is not seen with the native Mb which has three naturally occurring Tyr residues. Thus, the intensity increase observed for the mutant Mb is attributed to Tyr64. The corresponding bands of the *p*-cresol derivative exhibit greater intensity in polar (H-bond-forming) solvents than in nonpolar solvents. This result suggests that the increase in intensity of the Tyr bands in the transient form of the mutant myoglobin compared to that in the equilibrium form is due to exposure of Tyr64 to solvent water. Increased solvation indicates an outward movement of the phenol side chain and formation of an open channel to the distal pocket.

Introduction

Ligand binding to myoglobin (Mb) is one of the simplest chemical reactions carried out by proteins and provides basic information on rapid motions of globular proteins in respond to external stimuli.[1] X-ray crystallographic analysis of deoxy-Mb and carbonmonoxy-Mb (COMb) pointed out that there is no prepared pathway for migration of CO from the solvent to the buried binding site in the heme pocket, and accordingly, these structures have been referred to as "closed" forms.[2,3] Significant rearrangements of protein residues are required for ligand entry and release. Transient forms that generate a pathway between the binding site and the solvent are referred to as "open" forms.[2a]

When bulky ligands such as imidazole,[4a] phenyl anion,[4b] and ethyl isocyanide[4c] bind to the heme iron, His64 and Arg45 swing out of the heme pocket. This geometry allows small ligands to migrate from the binding site to the solvent, and accordingly, this structure has been regarded as a model of the "open" form. The CO binding modes of COMb have been categorized into substates (A_0−A_3) on the basis of infrared C−O stretching (ν_{CO})[5] and Raman Fe−CO stretching (ν_{Fe-CO}) frequencies which are inversely correlated.[6,7] The neutral A_1 (ν_{CO} = 1945 cm^{-1}, ν_{Fe-CO} = 507 cm^{-1}) and acidic A_0 (ν_{CO} = 1966 cm^{-1}, ν_{Fe-CO} = 488 cm^{-1}) substates of native Mb have been assigned to "closed" and "open" forms, respectively,[8,9] since at low pH the protonated form of the distal histidine rotates out into the solvent.[2c,8a,b] An open form of COMb can be generated at neutral pH by replacing Phe46(CD4) with Val.[10] This mutation creates a "hole" adjacent to the distal histidine allowing the imidazole side chain to rotate up and away from the bound ligand.

Previous time-resolved resonance Raman (TR^3) studies on the ν_{Fe-CO} band of recombined COMb indicated that the recombination rate as well as the static ν_{Fe-CO} frequency depends on the nature of residue 64.[11] Bimolecular recombination of CO with wild-type myoglobin begins around 1 μs following photolysis and reaches 60% at 1 ms,[12,13] but the ν_{Fe-CO} band corresponding to the open form has not been detected in a transient state before the appearance of the equilibrium ν_{Fe-CO} band.[14] To explore the reality of a transient open form, it seemed essential to examine the movements of residue 64 after photolysis and before ligand recombination.

Recently, it has become fairly easy to measure UV resonance Raman spectra excited in the 200−240 nm region.[15] UV resonance Raman (UVRR) spectroscopy gives structural information on proteins, particularly on aromatic residues, and is extensively used to elucidate higher-order structural changes involved in ligand binding of hemoglobin (Hb).[16,17] To apply this technique for monitoring the movement of residue-64, His64 was replaced with Tyr (H64Y) through site-directed mutagenesis, and its UV time-resolved resonance Raman (UV TR^3) spectra were obtained in this study. We succeeded in measuring the vibrational spectrum of the individual Tyr64 residue with nanosecond time resolution. The phenol side chain becomes more exposed to water immediately after photolysis, perhaps forming a transient open conformation.

[†] Okazaki National Research Institutes.
[‡] Rice University.
[§] Present address: Osaka University, Toyonaka, 560 Japan.
* To whom correspondence should be addressed.

S1089-5647(98)00070-4 CCC: $15.00
Published on Web 04/11/1998

Experimental Section

Native sperm whale Mb was isolated from stored meat according to Yamazaki et al.,[18] and the H64Y mutant was obtained as described previously.[19] About 0.5 mL of 400 μM Mb solution in 50 mM Tris-HCl buffer, pH 8.0, was put into a rubber-topped tube, while 50% (56% w/w) glycerol/water samples were obtained by mixing the Mb solution with an equal volume of glycerol. The deoxy form was obtained by adding sodium dithionite (1 mg/mL) to the Mb solution after replacement of the inside air of the tube with N_2 gas. The CO form was derived by the same procedure as for the deoxy form but under CO atmosphere. The 0.1 mL aliquot of the sample was transferred into a quartz spinning cell (diameter = 5 mm) with a microsyringe after the exchange of inside air of the cell with N_2 for the measurements of the deoxy form and with CO for the measurements of the CO form, respectively.[17c]

UV TR^3 spectra were measured with two 7 ns pulsed lasers operating at 30 Hz. The probe beam at 235 nm (20 μJ) was generated by frequency-doubling of the 470 nm output from an XeCl excimer laser-pumped dye laser (EMG 103MSC, 308 nm, and FL2002 using coumarine 480, Lambda Physik) with a β-BaB_2O_4 crystal. The pump beam (532 nm, 2 mJ) was the second harmonic of an Nd:YAG laser (Quanta-Ray, DCR-3). The pump and probe beams were made strictly collinear by a dichroic mirror, and the superimposed beams were line-focused onto the sample by two cylindrical lenses. The delay time (Δt) of the probe pulse from the pump pulse was controlled by a pulse generator (Stanford Research, DG-535) and was monitored on an oscilloscope (Tektronix, 2445B) by photodiode detection (Hamamatsu, S1722-02).

The pump and probe beams were introduced into the sample from the lower front side of the cell. The scattered light was collected with a Cassegrainian optics with *f*/1.1 and focused by a synthetic quartz lens onto an entrance slit of an asymmetric double monochromator (Spex 1404), in which the gratings in the first and second dispersion steps were 2400 (holographic) and 1200 grooves/mm (machine-ruled, 500 nm blaze),[17b] respectively, and detected by an intensified photodiode array (PC-IMD/C5222-0110G). The sample cell was rotated slowly (100 rpm) to avoid for two successive probe pulses to monitor an identical volume of the sample and also to allow for the photodissociated Mb to recombine with CO in one turn. The temperature of the sample solution was kept at 10 °C by flushing with cooled N_2 gas against the cell. One spectrum is composed of 400 exposures, each exposure accumulating the data for 0.8 s. The Raman spectra shown in the figures are averages of 4−10 spectra. The Raman shifts were calibrated with cyclohexane.

The visible TR^3 experiments were carried out as described previously.[14b] The probe beam at 416 nm was generated by the H_2-first Stokes shift of the third harmonic of an Nd:YAG laser (Quanta-Ray, DCR-3), and its power was made as low as possible (100 μJ/pulse) to avoid photodissociation by the probe pulse, while the pump beam (532 nm) was the same as described above. The sample cell was spun at 25 rpm, and the scattered light was dispersed with a triple polychromator (Spex1877) and detected with an intensified photodiode array (PAR, OMA III, 1421B). Reagent-grade 2,6-di-*tert*-butyl-*p*-cresol and spectrograde glycerol were used as purchased (Wako Pure Chemicals, Japan).

Results

Figure 1 shows the stationary-state UVRR spectra of native (a) and H64Y COMbs (b) excited at 235 nm and their difference

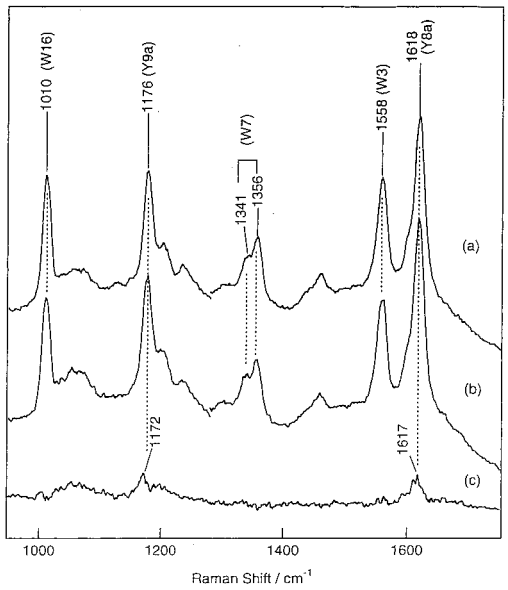

Figure 1. Stationary-state UVRR spectra of native sperm whale COMb (a) and H64Y COMb (b) excited at 235 nm and their difference (c) (= b − a). The Mb samples were equilibrated with 50 mM Tris-HCl buffer, pH 8.0; Mb concentration, 400 μM.

(c) (= H64Y − native) in the frequency region between 950 and 1700 cm^{-1}. In spectrum (a) the RR bands of Tyr are observed at 1176 (Y9a),[20] 1205 (Y7a), and 1618 cm^{-1} (Y8a) cm^{-1} and those of Trp at 1010 (W16),[20] 1341 and 1356 (W7 and Fermi doublet), and 1558 cm^{-1} (W3) cm^{-1}. In spectrum (c) the contribution from Tyr64 is seen for Y9a and Y8a bands, while Trp bands are completely canceled. Hereafter, Trp bands will be used as intensity standards for calculations of difference spectra. The weak features of difference peaks of Trp and Tyr residues in spectrum (c) suggest that the most of the Tyr and Trp bands are canceled since H64Y COMb adopts a structure similar to the native COMb. The differences can be solely attributed to replacement of His64 by Tyr. The Y8a and Y9a bands of Tyr64 in spectrum (c) appear broader and weaker than one-fourth of those in spectrum (b) expected if all four Tyr residues had equal intensities. This is partly due to inhomogeneous broadening, since Tyr64 may have more freedom in side chain orientation than those in helix parts. Practically the same kinds of results were obtained for the deoxy state.

Figure 2A (upper panel) displays the raw UV TR^3 spectra of native COMb in the region between 1150 and 1700 cm^{-1} observed for $\Delta t = -100$ (b), 0 (c), and 500 ns (d). Spectrum (a) was observed in the absence of the pump beam (hereafter referred as a "probe-only" spectrum). The lower panel (B) shows the differences of the pump/probe spectra with regard to the probe-only spectrum. The absence of any peaks in spectrum (a) indicates that the spectrum for $\Delta t = -100$ ns, which should reflect the spectrum after one turn of the spinning cell but before the next photolysis, is in agreement with the spectrum observed without the pump beam (probe-only). There are no features in spectra (b) and (c), suggesting that no spectral changes occur to Tyr and Trp residues of native Mb upon photodissociation of CO.

Figure 3 shows similar results of H64Y COMb measured with the same instrumental conditions (laser powers, exposure times, and accumulation times) as those used for Figure 2. In panel B, the differences with regard to the probe-only spectrum are delineated. No features are recognized in spectrum (a). However, in contrast with native Mb, clear peaks are identified at 1619 (Y8a) and 1177 cm^{-1} (Y9a) in spectra (b) and (c) for

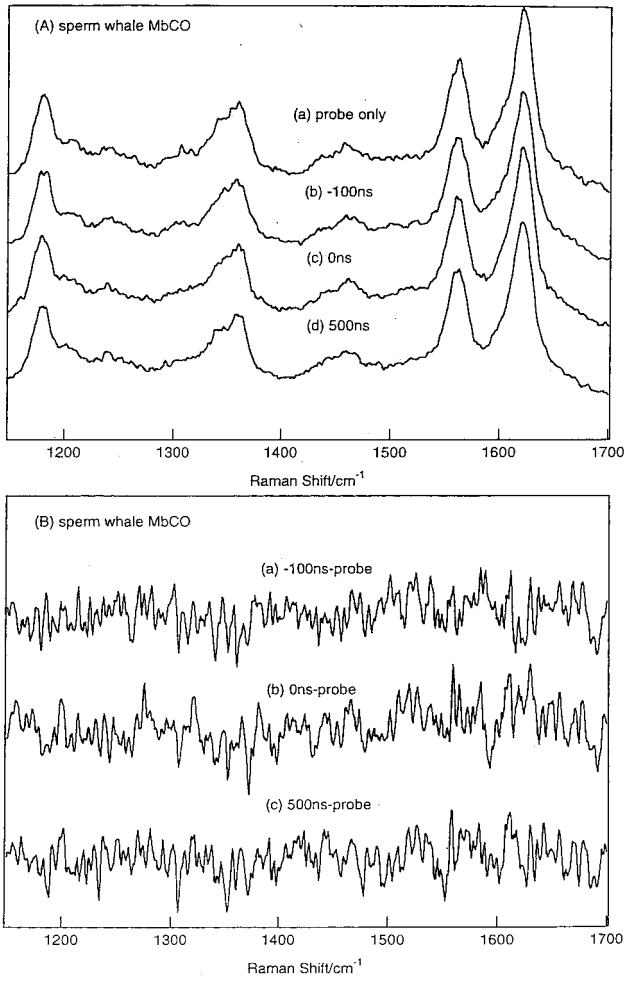

Figure 2. UV TR^3 spectra of native COMb probed at 235 nm. (A) Raw pump/probe spectra: (a) probe-only, (b) $\Delta t = -100$ ns, (c) $\Delta t =$ 0 ns, (d) $\Delta t = 500$ ns. (B) Difference spectra of the pump/probe spectra minus the probe-only spectrum: (a) $\Delta t = -100$ ns, (b) $\Delta t = 0$ ns, (c) $\Delta t = 500$ ns. Pump: 532 nm, 2 mJ/pulse. Probe: 235 nm, 20 μJ/pulse. Repetition: 30 Hz.

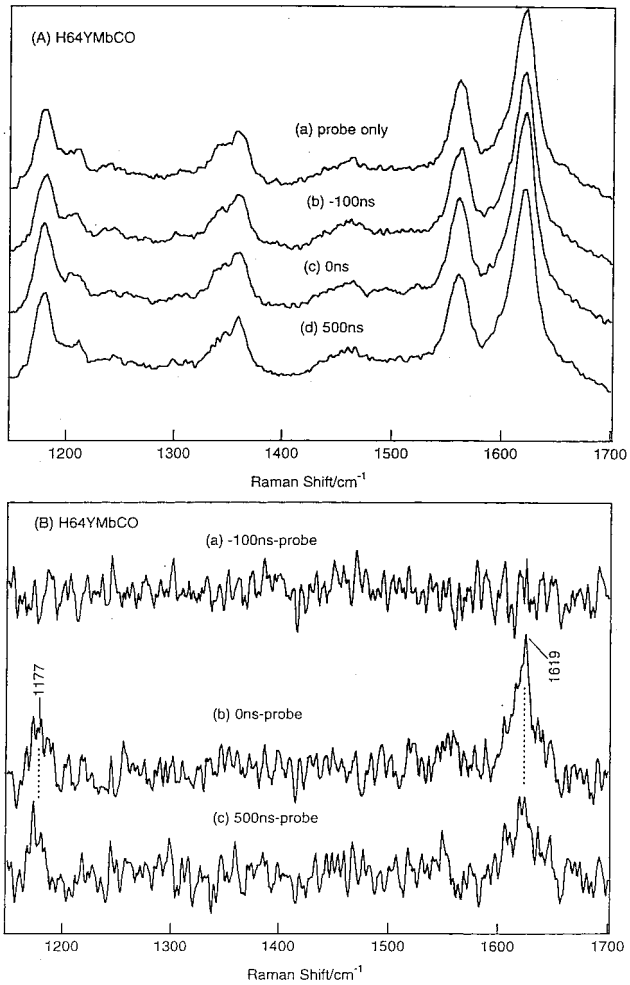

Figure 3. UV TR^3 spectra of H64Y COMb probed at 235 nm. (A) Raw pump/probe spectra: (a) probe-only, (b) $\Delta t = -100$ ns, (c) $\Delta t =$ 0 ns, (d) $\Delta t = 500$ ns. (B) Difference spectra of the pump/probe spectra minus the probe-only spectrum: (a) $\Delta t = -100$ ns, (b) $\Delta t = 0$ ns, (c) $\Delta t = 500$ ns. Pump: 532 nm, 2 mJ/pulse. Probe: 235 nm, 20 μJ/pulse. Repetition: 30 Hz.

H64Y COMb. These bands must be ascribed to Tyr64. To see time dependencies of intensity of these Tyr bands, the measurements were extended to longer delay times.

Figure 4 displays the differences of the pump/probe spectra of H64Y COMb with regard to the probe-only spectrum. The measurements were carried out with a sample different from that used for the measurements of Figure 3, and therefore reproducibility of the phenomenon was confirmed. The rise of Y8a and Y9a bands of Tyr is almost simultaneous with photodissociation in the present time resolution. The enhanced intensity lasts until 100 μs but thereafter gradually decays and completely disappears at 5 ms. To see the correlation between this spectral change and CO recombination, visible TR^3 experiments were carried out with the H64Y COMb.

Figure 5 shows the raw TR^3 spectra probed at 416 nm for H64Y COMb in the time range from -20 ns to 1 ms following photolysis. The equilibrium ν_{Fe-CO} RR band of H64Y COMb is observed at 491 cm^{-1} in the spectrum for $\Delta t = -20$ ns and, accordingly, is categorized into A_0. This band disappears in the spectrum for $\Delta t = 0$ ns, but a different band appears at 500 cm^{-1}. Due to the overlapping with this band, the intensity recovery of the equilibrium ν_{Fe-CO} RR band at 491 cm^{-1} is difficult to see in the raw spectra, while it seems to recover from $\Delta t = \sim 1$ μs. Therefore, band fitting calculations were carried out using two Lorentzian functions, and the results for four selected Δt's are illustrated in Figure 6, where the two assumed component bands and their sums are depicted with dotted and solid lines, respectively, and observed spectra are represented with thin solid lines. The good overlaps of the two solid lines mean that the assumed component bands correctly reflect the observed features.

The intensity of the 500 cm^{-1} band scarcely changes in the time range between 20 ns and 100 μs, during which the band at 491 cm^{-1} did not appear. The intensities of both bands increased with lapse of time after 100 μs, and at the same time, the intensity of the 500 cm^{-1} band relative to that of the 491 cm^{-1} band gradually decreased. The intensity of the 491 cm^{-1} band increased to 56% of the probe-only spectrum at $\Delta t = 1$ ms. After 1 ms, the absolute intensity of the 500 cm^{-1} band decreased slightly, although a frequency shift was not recognized during this process. The CO isotopic frequency shift was confirmed for the 491 cm^{-1} band but was not clear for the 500 cm^{-1} band. Therefore, the 500 cm^{-1} band might be a ν_{Fe-CO} mode of the geminately recombined COMb, but it is also highly possible that the 500 cm^{-1} band is a porphyrin band of a precursor species of the equilibrium COMb as observed for native and several mutant photolyzed COMb's.[14b] The time course of the UVRR spectral changes shown in Figure 4 is roughly compatible to that of the intensity increase of the equilibrium ν_{Fe-CO} RR band.

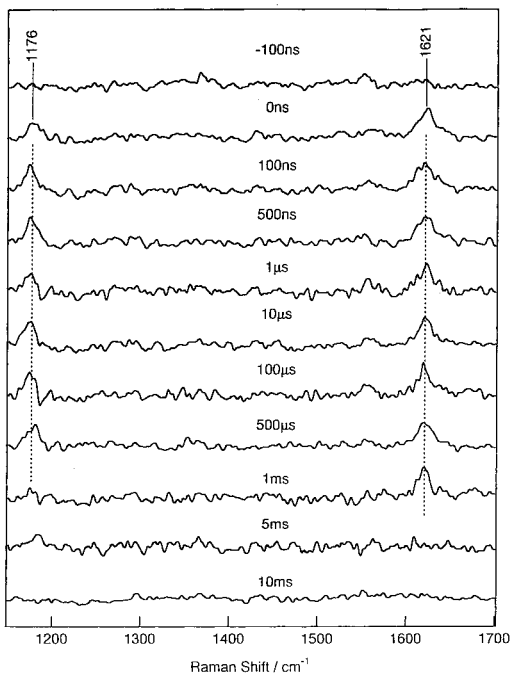

Figure 4. UV TR^3 spectra of H64Y COMb probed at 235 nm. The pump/probe spectra are represented in terms of the differences with regard to the probe-only spectrum. The delay times are specified in the figure for each spectrum. The instrumental conditions are the same as those in Figure 3.

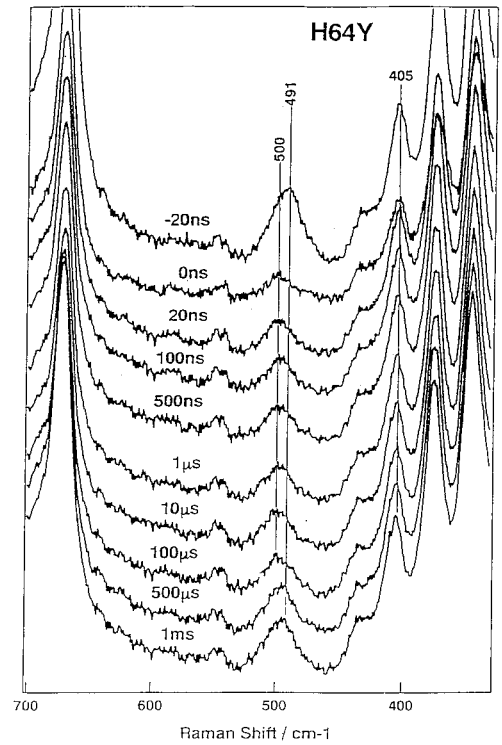

Figure 5. Visible TR^3 spectra in the ν_{Fe-CO} region of H64Y COMb in the range of Δt between −20 ns and 1 ms. Instrumental conditions: pump, 532 nm, 4 mJ; probe, 416 nm, 100 μJ; repetition, 10 Hz, accumulation time, 4000 s for each.

Figure 7 shows the results of UV TR^3 experiments obtained for H64Y COMb in 50% glycerol/water solution. The observed pump/probe spectra are represented in terms of the difference spectra with regard to the probe-only spectrum. The UVRR bands of Trp residues in the raw spectra were used as intensity standards in difference calculations. In this highly viscous

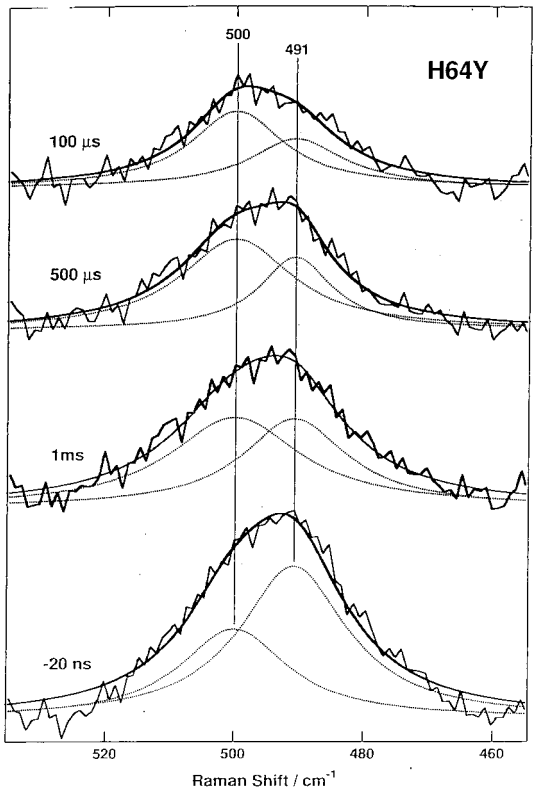

Figure 6. Band fitting calculations for the transient ν_{Fe-CO} bands of H64Y COMb with two Lorentzian functions using the least-squares method. The dotted lines denote individual component functions, and the solid lines denote the sum of the two-component functions. Thin solid lines are the observed spectra.

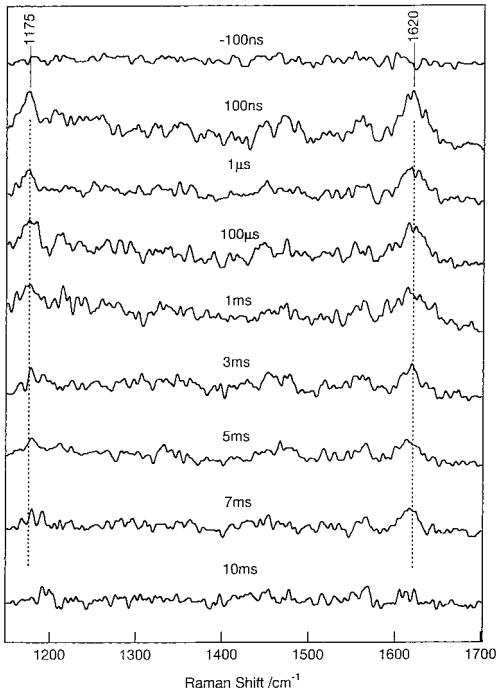

Figure 7. UV TR^3 spectra of H64Y COMb in the 50% glycerol/water solution probed at 235 nm. The pump/probe spectra are represented in terms of the differences with regard to the probe-only spectrum. The delay times are specified in the figure for each spectrum. The instrumental conditions are the same as those in Figure 3.

solution, the spectrum for $\Delta t = -100$ ns exhibits no features, indicating that everything is restored in one turn of the spinning cell (500 ms). The spectrum for $\Delta t = 100$ ns shows the bands

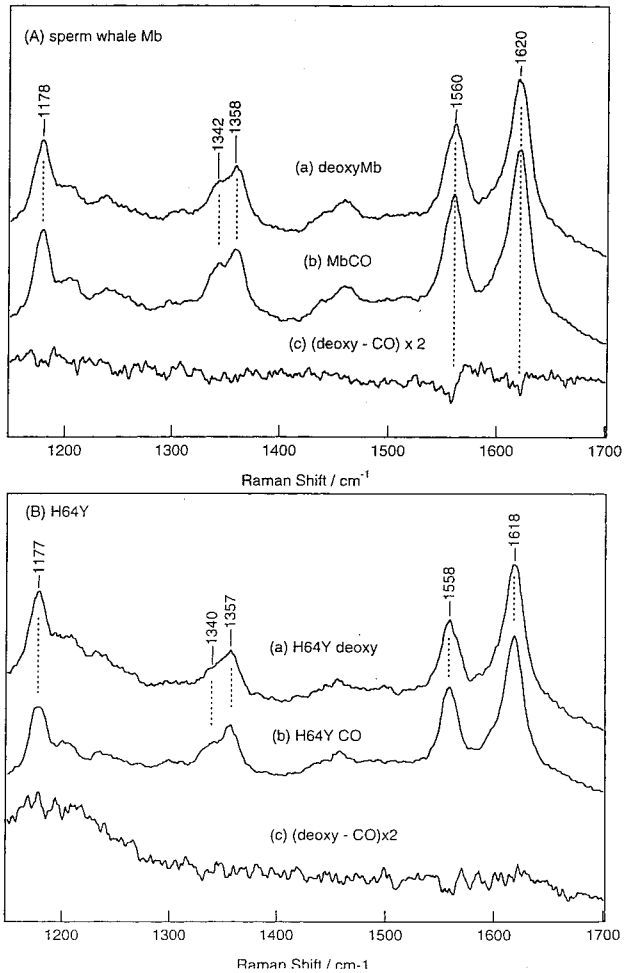

Figure 8. The stationary-state UVRR spectra of native Mb (A) and H64Y Mb (B) probed at 235 nm: (a) deoxy form, (b) CO-bound form, (c) difference spectrum, (deoxy − CO).

of Tyr at 1620 (Y8a) and 1175 cm^{-1} (Y9a), although they are broader than those in the absence of glycerol, probably owing to inhomogeneous broadening caused by slow changes of protein strucutres under high viscosity. These bands are still recognized in the spectrum for $\Delta t = 5$ ms when all features have disappeared in the absence of glycerol (Figure 4). In other words, the UVRR spectral recovery to the unphotolyzed state is significantly slow in the glycerol/water solution. This is consistent with the reported fact that the recombination rate of photodissociated CO becomes slower with increase of viscosity of the solution.[21] Consequently, it is reasonable to ascribe the appearance of UVRR bands of Tyr to a transient form present before CO recombination.

The differences between the stationary-state CO-bound and deoxy states were examined for both native and H64Y Mb's. Figure 8 shows the UVRR spectra of deoxy (a) and CO-bound (b) forms and their difference (deoxy − CO) of native (A) and H64Y Mb's (B). In the case of native Mb, the W3 band of Trp (1560 cm^{-1}) and the Y8a band of Tyr (1620 cm^{-1}) are slightly intensified in the CO-bound form, and accordingly, small troughs are seen in spectrum (c) of Figure 8A, but these are different from the features seen in Figure 2B. In the case of H64Y Mb, the relative intensities of the Tyr and Trp bands are different from those of native Mb, and such troughs are much weaker. Thus, the difference in UVRR intensities of Tyr and Trp bands between the CO-bound and deoxy stationary states is small and cannot be an origin for the transient spectral features observed in Figures 4 and 7.

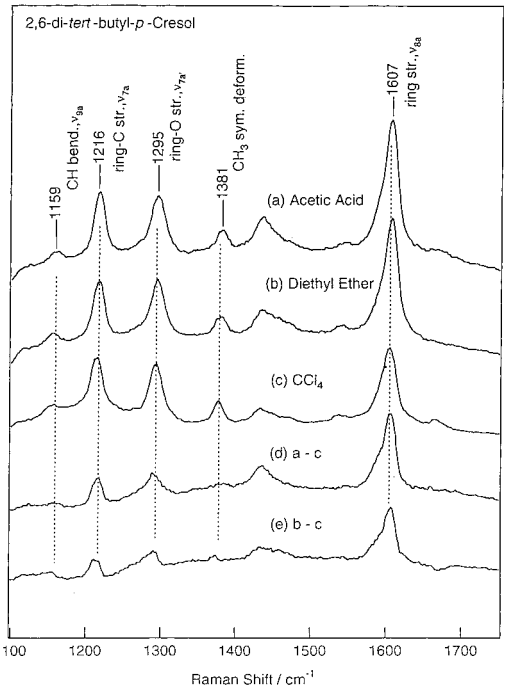

Figure 9. Solvent effects of the UVRR specta of 2,6-di-*tert*-butyl-*p*-cresol excited at 235 nm: (a) acetic acid, (b) diethyl ether, (c) CCl_4, (d) difference, (a) − (c), (e) difference, (b) − (c). The difference spectra are calculated so that the 1381 cm^{-1} band (CH_3 symmetric deformation mode) can be abolished. The bands are assinged according to ref 20b.

To understand the physical meaning of the appearance of these Tyr Raman bands in the transient state, solvent effects of UVRR spectra of *p*-cresol were examined previously. The intensities of Y8a and Y9a bands were significantly stronger in the hydrogen-bond-forming solvents than in the non-hydrogen-bonding solvents.[17e] However, there might be an argument against it, because the observed effects arise from the dimer formation of *p*-cresol in hydrophobic solvents. Therefore, solvent effects of 2,6-di-*tert*-butyl-*p*-cresol, which cannot make a dimer due to steric hindrances between bulky *tert*-butyl groups, were investigated in this study. Figure 9 shows the 235 nm excited Raman spectra of 2,6-di-*tert*-butyl-*p*-cresol in acetic acid (a), diethyl ether (b), carbon tetrachloride (c), and their difference spectra; (d) = (a) − (c), and (e) = (b) − (c). Acetic acid and diethyl ether serve as a hydrogen-bond donor and acceptor, respectively, while in CCl_4 no hydrogen bond would be formed. The difference spectra were calculated so that the CH_3 deformation band at 1381 cm^{-1} could be abolished. It is evident from spectra (d) and (e) that the intensity of the 1607 cm^{-1} band (ν_{8a}) increases in hydrogen-bond-forming solvents compared with that in non-hydrogen-bond-forming solvent (CCl_4), in agreement with the previous results for *p*-cresol.[17e] The 1159 cm^{-1} band (ν_{9a}) also exhibits a similar trend, although this band is weaker than ν_{7a} and $\nu_{7a'}$.

The results for the model compounds suggest that the intensity of Y8a and Y9a bands of Tyr would be stronger if the Tyr is placed in hydrophilic environments (more precisely, in hydrogen-bond-forming solvent) than in hydrophobic environments. As described above, the transient Tyr bands observed in Figures 4 and 7 arise from Tyr64. Therefore, the stronger UVRR intensities of the Y8a and Y9a bands of H64Y Mb in the transient state mean that Tyr64 is exposed to water during that time, but when it returns into the heme pocket, the Raman intensity becomes weaker, similar to the case of nonpolar solvents irrespective of the presence or absence of CO.

Discussion

It was anticipated from the X-ray crystallographic analysis of the imidazole-, phenyl anion-, and ethyl isocyanide-bound Mb's,[4] that His64 together with Arg45 swings out of the heme pocket in the open form. Recent X-ray analysis on acidic Mb[2c] has demonstrated that His64 adopts the swung-out geometry upon its protonation. The ν_{Fe-CO} RR band of COMb exhibited a frequency shift from 507 cm^{-1} at pH 7 to 488 cm^{-1} at pH 4.1,[9] and these ν_{Fe-CO} frequencies were correlated with the stationary "closed" and "open" structures, respectively. However, in the transient resonance Raman studies for recombination process of CO following photodissociation of COMb,[11,14] a transient ν_{Fe-CO} band was not detected around 490 cm^{-1} prior to the appearance of the equilibrium ν_{Fe-CO} band around 510 cm^{-1}. To pursue possible rapid movements of His64, this residue was replaced by a UVRR active Tyr in this study.

The vibrational frequencies of Tyr and Trp are generally sensitive to surroundings.[20a] In fact, some bands of Trp and Tyr in the UVRR spectra of Hb excited at 235 nm[17d,e] exhibit appreciable sensitivity to higher-order structural changes. There are three Tyr (103, 146, and 151), and two Trp (7 and 14) residues in native sperm whale Mb. Since the two Trp residues (A6 and A12) and one Tyr (G4) are contained in the helix part and the remaining Tyr residues are at the end of the chain (HC2 and HC7), their surroundings are little altered by ligand binding. These Tyr residues give rather sharp UVRR bands, and their intensity differences between the deoxy and CO-bound forms are negligibly small (Figure 8A). The UVRR spectra of the deoxy and CO-bound forms of H64Y Mb are also alike (Figure 8B), indicating that the environment of Tyr64 is not greatly altered by the presence or absence of CO. As long as Tyr64 lies within the heme pocket, the UVRR band of Tyr64 appears weaker and broader than those of three Tyr residues (Figure 1), presumably due to appreciable inhomogeneity of its immediate surroundings.

In native deoxy-Mb, a water molecule stays in the heme pocket, but the water molecule is missing in the CO-bound form.[22] It is not clear whether a water molecule is present in the heme pocket of H64Y deoxy-Mb. However, if present, such a water molecule does not cause significant changes in UV Raman properties of Tyr64 since there are little spectral differences between H64Y COMb and H64Y deoxy-Mb. The results shown in Figures 4 and 7 demonstrate the generation of a more polar atmosphere around Tyr64 of H64Y COMb immediately after photolysis and its continuation until recombination.

The Y8a and Y9a bands of Tyr are mainly associated with the ring C═C stretching and in-plane C−H bending vibrations, respectively.[20b] Y7a at 1210 cm^{-1} and Y7a′ at 1263 cm^{-1}, which are mainly associated with the CH_2-C_{ring} and $HO-C_{ring}$ stretching modes, respectively,[20b] should be sensitive to hydrogen bonding, and recent experiments on O-phosphorylation of Tyr noted a frequency shift of Y7a′,[23] but these bands of Mb are weaker and not resolved in the transient spectra. On the other hand, Y8a and Y9a are strong, and their intensities are dependent on the excitation wavelength.[24] When the surroundings of Tyr are altered, the absorption maxima due to the L_a (222 nm) and L_b (273 nm) transitions would be influenced, and as a result UVRR intensity would be altered. In fact, these bands of *p*-cresol are significantly stronger in hydrogen-bond-forming solvents than in non-hydrogen-bond-forming solvents.[17e] The results shown in Figure 9 demonstrate that the intensity change is not caused by dimer formation. Therefore, the stronger intensity of Y8a and Y9a bands of Tyr in the transient state suggests that Tyr64 is placed in the hydrogen-bond-forming (or hydrophilic) surroundings. Accordingly, it is very likely that Tyr64 is exposed to solvent in the transient state.

There might be an argument that water molecules transiently come into the heme pocket. If water molecules are present inside the photodissociated deoxy heme pocket and form internal hydrogen bonds with Tyr, they must go out of the heme pocket when CO comes in. In such a case, the same UVRR spectral change as observed for transient states should be observed between the stationary liganded and unliganded states. This is contradictory to the observation that there is little difference between the stationary UVRR spectra of Tyr in the equilibrium CO-bound and deoxy forms (Figure 8B). Furthermore, the time period in which Tyr64 is in a polar environment is longer when glycerol is present. Since glycerol is too big to enter the distal pocket, it can only influence the transient changes by osmotically removing water from the protein or inhibiting protein motions by increasing solvent viscosity. The latter phenomenon appears to be occurring, keeping the Tyr64 side chain in an "open" conformation longer after photolysis. Osmotic removal of water from a closed conformation would prevent formation of a more polar transient deoxy structure and not increase its lifetime.

Molecular dynamics simulations[25] indicate that His64 takes the position of the open form occasionally in the equilibrium state, but its probability is very low. A small fraction of open forms may be present at equilibrium in H64Y deoxy- and CO-myoglobin. However, our present experiments demonstrate that the population of the open form becomes considerably larger immediately after photodissociation. This could be caused by strong collision between Tyr64 and photodissociated CO which has the large kinetic energy of gas molecules of a bomb blast in a confined space. The increment of additional open form due to the pressure of photodissociated CO corresponds to the difference in intensities of the Tyr bands in Figures 4 and 7. Even if a small amount of open conformation is present in the stationary deoxy and CO forms, its contributions are small and roughly the same in both complexes as judged by the difference spectra in Figures 4 and 7.

In conclusion, the present UV TR^3 experiments with H64Y Mb demonstrate the presence of the transient conformation in which Tyr64 swings out of the heme pocket and is exposed to solvent, presumably creating a channel from the solvent to the ligand binding site. This structure lasts as long as 1 ms in an ordinary aqueous solution and much longer in glycerol/water mixtures.

Acknowledgment. This work was partly supported by grants from the United States National Institutes of Health GM35649 and HL47020, The Robert A. Welch Foundation Grant C-612, and the W. M. Keck Center for Computational Biology, and also by Grant-in-Aids for Scientific Research on Priority Areas (08249106) from the Ministry of Education, Science, Sports and Culture, Japan.

References and Notes

(1) Frauenfelder, H.; Sligar, S. G.; Wolynes, P. G. *Science* **1991**, *254*, 1598−1603.

(2) (a) Springer, B. A.; Sligar, S. G.; Olson, J. S.; Phillips, G. N., Jr. *Chem. Rev.* **1994**, *94*, 699−714. (b) Olson, J. S.; Phillips, G. N., Jr. *J. Biol. Chem.* **1996**, *271*, 17593−17596. (c) Yang, F.; Phillips, G. N., Jr. *J. Mol. Biol.* **1996**, *256*, 762−774. (d) Schlichting, I.; Berendzen, J.; Phillips, N. J., Jr.; Sweet, R. M. *Nature* **1994**, *371*, 808−812.

(3) Kuriyan, J.; Wilz, S.; Karplus, M.; Petsko, G. A. *J. Mol. Biol.* **1986**, *192*, 133−154.

(4) (a) Bolognesi, M.; Cannillo, E.; Ascenzi, P.; Giacometli, G. M.; Merli, A.; Brunori, M. *J. Mol. Biol.* **1982**, *158*, 305−315. (b) Ringse, D.; Petsko, G. A.; Kerr, D.; Ortiz de Montellano, P. R. *Biochemistry* **1984**, *23*,

2−4. (c) Johnson, K. A.; Olson, J. S.; Phillips, G. N., Jr. *J. Mol. Biol*. **1989**, *207*, 459−463.

(5) (a) Makinen, M. W.; Houtchens, R. A.; Caughey, W. S. *Proc. Natl. Acad. Sci. U.S.A.* **1979**, *76*, 6042−6046. (b) Tsubaki, M.; Srivastava, R. B.; Yu, N.-T. *Biochemistry* **1982**, *21*, 1132−1140. (c) Ansari, A.; Berendzen, J.; Braunstein, D.; Cowen, B. R.; Frauenfelder, H.; Hong, M. K.; Iben, E. T.; Johnson, J. P.; Ormos, P.; Sauke, T. B.; Scholl, R.; Schulte, A.; Steinbach, P. J.; Vittitow, J.; Young, R. D. *J. Biophys. Chem.* **1987**, *26*, 337−355. (d) Frauenfelder, H.; Park, F.; Young, R. D. *Annu. Rev. Biophys. Chem*. **1988**, *17*, 451−479.

(6) Li, X.-Y.; Spiro, T. G. *J. Am. Chem. Soc*. **1988**, *110*, 6024−6033.

(7) Li, T.; Quillin, M. L.; Phillips, G. N., Jr.; Olson, J. S. *Biochemistry* **1994**, *33*, 1433−1446.

(8) (a) Morikis, D.; Champion, P. M.; Springer, B. A.; Sligar, S. G. *Biochemisty* **1989**, *28*, 4791−4800. (b) Sage, J. T.; Morikis, D.; Champion, P. M. *Biochemistry* **1991**, *30*, 1227−1236.

(9) Ramsden, J.; Spiro, T. G. *Biochemistry* **1989**, *28*, 3125−3128.

(10) Lai, H. H.; Li, T.; Lyons, D. S.; Phillips, G. N., Jr.; Olson, J. S.; Gibson, Q. H. *Proteins: Struct. Funct. Genet*. **1995**, *22*, 322−339.

(11) (a) Sakan, Y.; Ogura, T.; Kitagawa, T. *Chem. Phys. Lett*. **1992**, *196*, 150−154. (b) Sakan, Y.; Ogura, T.; Kitagawa, T. *Biochemistry* **1993**, *32*, 5815−5824.

(12) (a) Henry, E. R.; Sommer, J. H.; Hofrichter, J.; Eaton, W. A. *J. Mol. Biol*. **1983**, *166*, 443−451. (b) Balasubramanian, S.; Lambright, D. G.; Simmons, J. H.; Gill, S. J.; Boxer, S. G. *Biochemistry* **1994**, *33*, 8355−8360. (c) Ansari, A.; Jones, C. M.; Henry, E. R.; Hofrichter, J.; Eaton, W. A. *Biochemisty* **1994**, *33*, 5128−5145. (d) Steinbach, P. J.; Ansari, A.; Berendzen, J.; Braunstein, D.; Chu, K.; Cowen, B. R.; Ehrenstein, D.; Frauenfelder, H.; Johnson, J. B.; Lamb, D. C.; Luck, S.; Mourant, J. R.; Nienhaus, G. U.; Ormos, P.; Philipp, R.; Xie, A.; Young, R. D. *Biochemistry* **1991**, *30*, 3988−4001. (e) Nienhaus, G. U.; Mourant, J. R.; Frauenfelder, H. *Proc. Natl. Acad. Sci. U.S.A.* **1992**, *89*, 2902−2906. (f) Mourant, J. R.; Branstein, D. P.; Chu, K.; Frauenfelder, H.; Nienhaus, G. U.; Ormos, P.; Young, R. D. *Biophys. J.* **1993**, *65*, 1496−1507.

(13) Traylor, T. G.; Magde, D.; Taube, D. J.; Jongward, K. A.; Bandyopadhyay, D.; Luo, J.; Walda, K. N. *J. Am. Chem. Soc*. **1992**, *114*, 417−429.

(14) (a) Nakashima, S.; Kitagawa, T. *J. Am. Chem. Soc*. **1994**, *116*, 10318−10319. (b) Nakashima, S.; Kitagawa, T.; Olson, J. S. *Chem. Phys.*, in press.

(15) (a) Asher, S. A.; Bormett, R. W.; Chen, X. G.; Lemmon, D. H.; Cho, N.; Peterson, P.; Arrigon, M.; Spinelli, L.; Cannon, J. *Appl. Spectrosc*. **1993**, *47*, 628−633. (b) Kitagawa, T. *Prog. Biophys. Mol. Biol.* **1992**, *58*, 1−18.

(16) Rodgers, K. R.; Spiro, T. G. *Science* **1994**, *265*, 1697−1699.

(17) (a) Kaminaka, S.; Ogura, T.; Kitagawa, T. *J. Am. Chem. Soc*. **1990,** *112*, 23−27. (b) Kaminaka, S.; Kitagawa, T. *J. Am. Chem. Soc*. **1992**, *114*, 3256−3260. (c) Kaminaka, S.; Kitagawa, T. *Appl. Spectrosc*. **1995**, *49*, 685−687. (d) Nagai, M.; Kaminaka, S.; Ohba, Y.; Nagai, Y.; Mizutani, Y.; Kitagawa, T. *J. Biol. Chem*. **1995**, *270*, 1636−1642. (e) Nagai, M.; Imai, K.; Kaminaka, S.; Mizutani, Y.; Kitagawa, T. *J. Mol. Struct*. **1996**, *379*, 65−75.

(18) Yamazaki, I.; Yokota, K.; Shikama, K. *J. Biol. Chem*. **1964**, *239*, 4151−4153.

(19) (a) Carver, T. E.; Brantley, R. E., Jr.; Singleton, E. W.; Arduni, R. M.; Quillin, M. L.; Phillips, G. N., Jr.; Olson, J. S. *J. Biol. Chem*. **1992**, *267*, 14443−14450. (b) Springer, B. A.; Sligar, S. G. *Proc. Natl. Acad. Sci. U.S.A.* **1987**, *84*, 8961−8965. (c) Egenerg, K. D.; Springer, B. A.; Martinis, S. A.; Sligar, S. G.; Morikis, D.; Champion, P. M. *Biochemistry* **1990**, *29*, 9783−9791.

(20) (a) Harada, I.; Takeuchi, H. In *Spectroscopy in Biological Systems*; Clark, R. J. H., Hester, R. E., Eds.; John Wiley & Sons: Chichester, 1986; pp 113−176. (b) Takeuchi, H.; Watanabe, N.; Harada, I. *Spectrochim. Acta* **1988**, *44A*, 749−761.

(21) Balasubramanian, S.; Lambright, D. G.; Marden, M. C.; Boxer, S. G. *Biochemistry* **1993**, *32*, 2202−2212.

(22) Quillin, M. L.; Arduini, R. M.; Olson, J. S.; Phillips, G. N., Jr. *J. Mol. Biol*. **1993**, *234*, 140−155.

(23) Okishio, N.; Fukuda, R.; Nagai, M.; Nagai, Y.; Nagatomo, S.; Kitagawa, T. *J. Raman Spectrosc*. **1998**, *29*, 31−39.

(24) (a) Raba, R. P.; Spiro, T. G. *J. Phys. Chem*. **1985**, *89*, 1856−1861. (b) Asher, S. A.; Ludwig, M.; Johnson, C. R. *J. Am. Chem. Soc*. **1986**, *108*, 3186−3197.

(25) Jewsbury, P.; Kitagawa, T. *Biophys. J*. **1994**, *67*, 2236−2250.